Central European Journal of Energetic Materials
ISSN 1733-7178; e-ISSN 2353-1843

Cent. Eur. J. Energ. Mater. 2021, *18*(3): 385-404; DOI 10.22211/cejem/142604
Article is available in PDF-format, in colour, at:
https://ipo.lukasiewicz.gov.pl/wydawnictwa/cejem-woluminy/vol-18-nr-3/

Research paper

Tuning the Laser Ignition Properties of Nitrocellulose-Nitroglycerine-Hexogen Propellants via Incorporation of Carbon Nanotubes

Xianrui Shi[1,2], **Yongjie Jia**[2], **Linyu Chen**[3], **Lu Tian**[1], **Jinpeng Shen**[1], **Chonghua Pei**[1,*]

[1] *College of Materials Science and Engineering, Southwest University of Science and Technology, Mianyang 621010, China*
[2] *Xi'an Modern Chemistry Research Institute, Xi'an 710065, China*
[3] *School of Information Engineering, Southwest University of Science and Technology, Mianyang 621010, China*
* *E-mail:* peichonghua@swust.edu.cn

Abstract: Near infrared laser ignition is challenging owing to the poor near infrared laser absorption of nitrocellulose-nitroglycerine-hexogen (NC-NG-RDX) propellants. Less than 1 wt.% of carbon nanotubes (CNTs) were uniformly dispersed into the NC-NG-RDX propellants to tune its near infrared laser ignition property. The effects of CNTs on the thermal decomposition, near infrared light absorption and thermal conductivity of NC-NG-RDX propellants were studied. The near infrared laser ignition property of NC-NG-RDX propellants doped with CNTs were investigated compared with raw NC-NG-RDX propellant. The decomposition property and thermal conductivity of NC-NG-RDX propellants doped with CNTs were little changed due to the small quantity of CNTs. The laser reflectivity of the composite propellants decreased obviously as the content of CNTs was increased because of the high laser absorption property of CNTs. The laser ignition performance of the composites propellants is substantially improved by the incorporation of 0.5 wt.% or less CNTs and the successful ignition time decreases remarkably. Higher CNT content, such as 0.75 wt.% can lead to failure of laser ignition due to the excessive laser absorption efficiency and heating rate of the radiated region of the composite propellants together with inefficient deflagration. Our research reveals that the appropriate proportion of CNTs can potentially be used as a laser sensitizer for realizing effective infrared laser ignition of NC-NG-RDX propellants.

Keywords: nitrocellulose-nitroglycerine-hexogen propellants, NC-NG-RDX propellants, multi-walled carbon nanotubes, CNTs, light absorption, photothermal conversion, laser ignition

1 Introduction

Since the first laser device was developed in 1960, laser ignition of energetic materials has been a topic of interest [1-4] and become one of the most important ignition technologies in various weapon systems [5, 6]. At present, the laser ignition of energetic materials has been deepened and remarkable achievements have been made [7-10]. Nitrocellulose-nitroglycerine-hexogen (NC-NG-RDX) propellants are a traditional composite energetic material, which is composed of nitrocellulose (NC), nitroglycerin (NG) and cyclotrimethylenetrinitramine (RDX), and it is widely applied in solid rocket motors and artillery weapon systems due to its high energy, outstanding low smoke, excellent process performance and aging resistance [11-13]. However, NC and RDX have both been verified to be insensitive to light [14, 15], especially in the near infrared. There has therefore been a continuing need to improve the laser sensitivity of NC-NG-RDX composite propellants.

In order to increase the laser sensitivity of energetic materials, many approaches are being developed, such as improving the laser energy density, increasing the ambient pressure, and altering the formula of the energetic materials [16-19]. Among these approaches, improving the laser sensitivity of energetic materials is one of the most efficient and convenient ways. Therefore, a small amount of laser sensitive additives, such as graphene oxide [15, 20, 21], carbon black [18], graphite [22], and gold nanoparticles [23], have been incorporated into energetic materials to improve the controllability of laser ignition. Carbon nanotubes (CNTs) are an example of one-dimensional carbon nano-materials, which are widely used in various applications due to their special structure and outstanding mechanical and electrical properties [24, 25]. Recently, research has indicated that CNTs can absorb light energy and subsequently generate and transfer heat rapidly, and also show high photothermal efficiency [26-28]. CNTs also have been further used as optical ignition promoters in the fabrication of high-performance energetic materials, such as multi-walled CNTs/Al/CuO composites [29], single-walled CNTs/Al/CuO composites [30] and single-walled CNTs/PETN [31]. Therefore, CNTs could be another potential optically sensitive additive which could significantly improve the laser ignition performance of NC-NG-RDX propellants at a relatively low CNT content.

In this paper, NC-NG-RDX (40 wt.% RDX) propellants with different CNT contents were prepared by a kneading-extrusion method [32, 33]. The microstructure and thermal decomposition behavior of propellants containing CNTs were studied using scanning electron microscopy (SEM) and differential scanning calorimetry (DSC). Then the effect of CNTs on the light absorption behavior and thermal conductivity of the propellants were discussed. The results showed that the laser ignition efficiency of the propellants obviously depends on the CNT contents. The detailed laser ignition mechanism of the NC-NG-RDX propellants can be well described.

2 Materials and Methods

2.1 Materials preparation

The NC-NG propellant tablets from Sichuan Nitrocell Co., Ltd. (Sichuan, China) are composed of NC (12.6% nitrogen), NG and *N*,*N*'-dimethyl-*N*,*N*'-diphenylurea (Centralite). RDX was purchased from Gansu Yinguang Chemical Industry Group Co., Ltd (Gansu, China). The average particle diameter of RDX is 30 μm. In order to make CNTs disperse homogeneously in the composite propellants, hydroxyl functional multiwall carbon nanotubes (CNTsOH) were selected. The NC-NG-RDX based propellants were processed by a solvent method [32] with consistent parameters. Acetone/ethanol solvent (50:50 by volume) was employed for the propellant processing, in which solvent quantity was consistently 22 wt.% of the total solid mass. Firstly, different weight percentages of CNTsOH (3 wt.% –OH, 10~20 nm in diameter and 20~30 nm in length, Times Nano, Chengdu, China) and acetone/ethanol (Kelong, Chengdu, China) were mixed to disperse the CNTs by magnetic stirring for 30 min followed by sonicating for 30 min. Then NC-NG propellants tablets and RDX powders were mixed and kneaded in a 2.5 L mixer together with the CNTs/solvent solution for 3.5 h in order to make the RDX and CNTs disperse well. Lastly, the propellant doughs were extruded using a pressure of 10 MPa, and dried to obtain compact and desiccated propellant samples which are shown in the inserts in Figures 2(b) and 2(c). The propellants are composed of NC, NG, RDX and Centralite, CNTs being added as an extra. The detail of the composition of the propellants are shown in Table 1.

Table 1. The composition of NC-NG-RDX propellants with carbon nanotubes

Sample	NC [wt.%]	NG [wt.%]	Centralite [wt.%]	RDX [wt.%]	Additional CNTs [wt.%]
1	39.5	19	1.5	40.0	0
2					0.25
3					0.50
4					0.75

2.2 Materials characterization

The morphology and dimensions of the composite propellants were measured using SEM (JSM-5800S) at an acceleration voltage of 10-15 kV after gold sputtering coating under a vacuum of 10^{-6} Pa for 120 s. The density of the propellants was measured using the Bottle Method according to China's national military standard (GJB-770B-2005). The pore structure of the propellants was investigated using mercury porosimetry (AutoPore IV 9500). The thermal properties were measured using DSC-TG (NETZSCH STA 449C, Germany), recording with 50 mL/min N_2 at 10 K/min from 30 to 350 °C.

The light absorption property of the composite propellants was measured using a UH4150 UV-Visible/NIR spectrophotometer in the range of 400-2500 nm with a scan speed of 2400 nm/min. The thermal conductivity of the propellants was measured at 20 K/min using a NETZSCH LFA 447 Nanoflash™ instrument. The environmental temperature and humidity were 25 °C and 70%. The thickness and diameter of these samples were 1.0 and 12.7 mm, respectively.

The laser ignition properties of the propellants in an air atmosphere at 25 °C were studied using a self-built platform according to the schematic diagram reported by Herreros and Fang [34], and the scheme of laser ignition setup is shown in Figure 1. All samples with dimensions of 1.8×3.0×10.0 mm were ignited by a diode laser system (50 W, 800 nm) at 25 °C. The laser spot diameter is about 3 mm. The samples were positioned horizontally and the laser beamed vertically onto the surface of the samples. Considering the different ignition performance of the samples, a manual ignition pulse time was given in the experiment until deflagration occurred and successful ignition of the propellants realized.

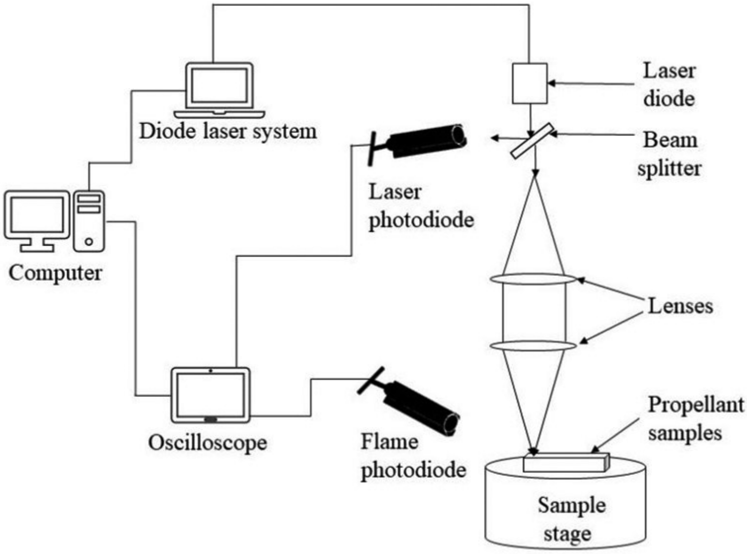

Figure 1. The scheme of our laser ignition experimental setup

3 Results and Discussion

3.1 Morphology characterizations

Figure 2 represents the microstructure of raw CNTs and NC-NG-RDX propellants. As shown in Figure 2(a), the raw CNTs have average diameters from 20 to 50 nm and lengths ranging from 5 to 50 µm. Figure 2(b) shows the microstructure of NC-NG-RDX propellant without CNTs. It was found that most of RDX particles with sizes of 5-20 µm were embedded the NC-NG matrix. Some RDX particles were pulled out after brittle fracture in liquid nitrogen. CNTs can be observed clearly at the fracture section of the 0.75 wt.% CNTs doped propellants at a larger magnification level (Figure 2(d)), and it is homogenously mixed with NC-NG matrix. However, the microstructure of the propellant with 0.75 wt.% CNTs (Figure 2(c)) displays no obvious change compared with the raw propellant. In addition, no obvious pore is introduced into the propellants due to the extrusion pressure up to 10 MPa. Their densities were about 1.63 g/cm^3. The propellants also had similar appearances according to the inserted photographs in Figures 2(b) and 2(c). Therefore, the addition of a small amount of CNT does not change the inner and surface structure of NC-NG-RDX propellants.

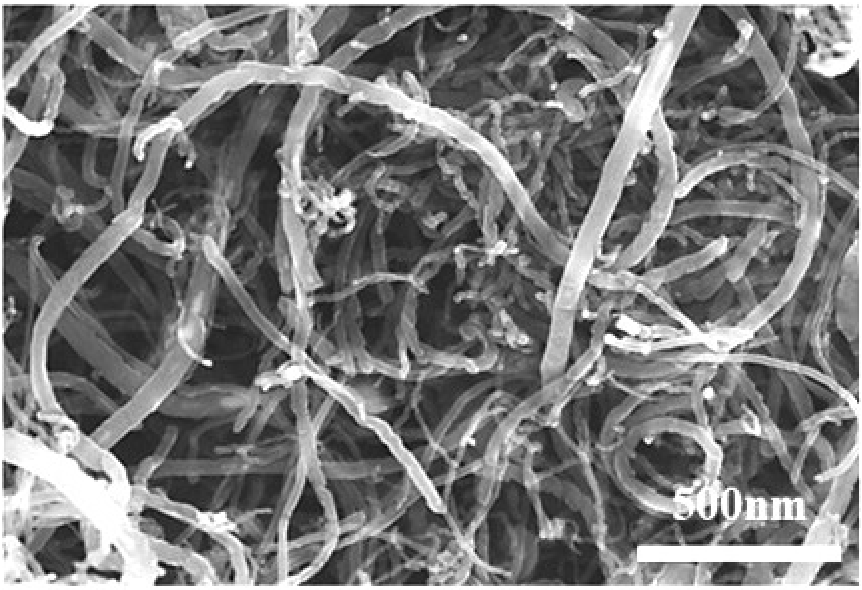

(a)

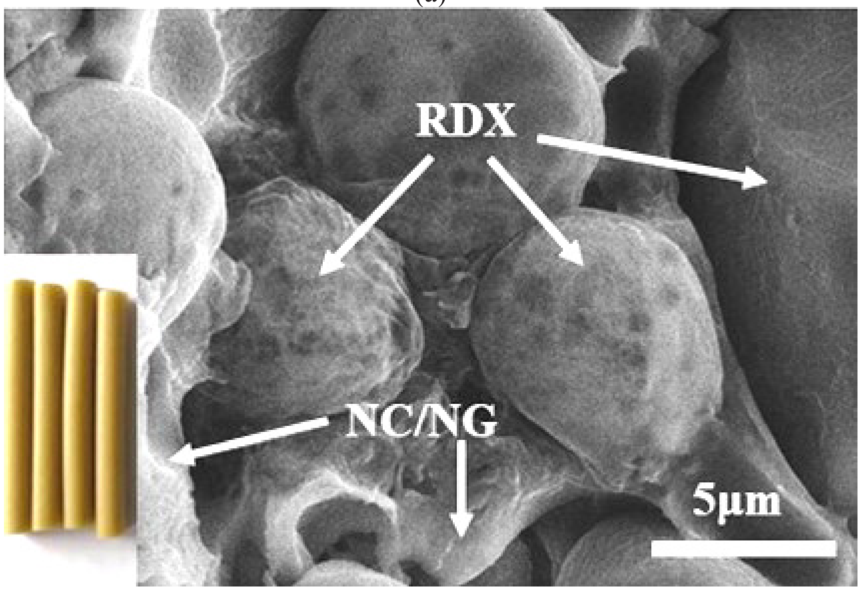

(b)

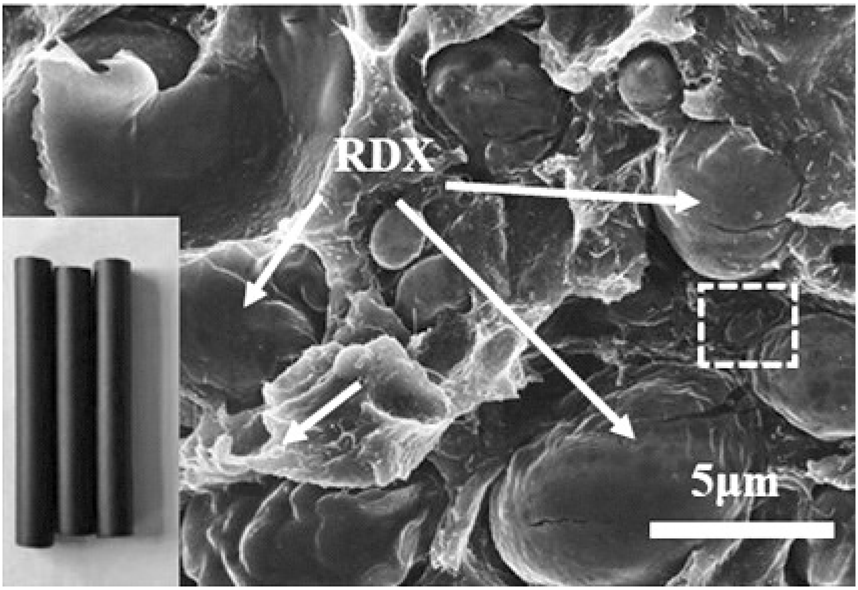

(c)

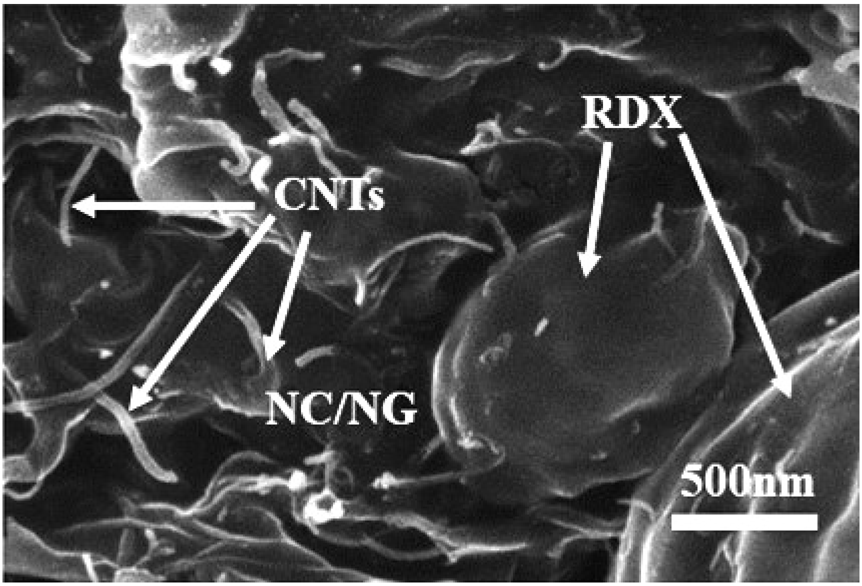

(d)

Figure 2. SEM images of raw CNTs (a), NC-NG-RDX propellant (b) and 0.75 wt.% CNTs doped NC-NG-RDX propellants (c, d)

3.2 Thermal decomposition property

The thermal decomposition processes of NC/NG, RDX and NC-NG-RDX propellants were investigated using DSC analysis, and the results are shown in Figure 3. NC/NG and RDX both show each a single exothermic peak at 201 and 253 °C, respectively. However, RDX shows an endothermic peak at 204 °C due to it melting at that temperature. The DSC curve for NC-NG-RDX propellants shows two exothermic peaks at 201.8 and 229.5 °C, which represents the decomposition of the NC/NG matrix and the RDX particles, respectively [35]. As can be seen, the exothermic peak temperature of RDX in NC-NG-RDX propellant is 23.5 °C lower than that of RDX powder. So, the thermal stability of RDX is reduced by the decomposition of NC/NG. However, the melting ability of RDX before decomposition cannot be changed, though the melting process of RDX cannot be observed in the DSC curve of NC-NG-RDX propellant. Furthermore, as shown in Figure 3, compared with raw NC-NG-RDX propellant, no obvious change of decomposition performance is found for NC-NG-RDX propellant doped with CNTs due to the low content of CNTs that were incorporated.

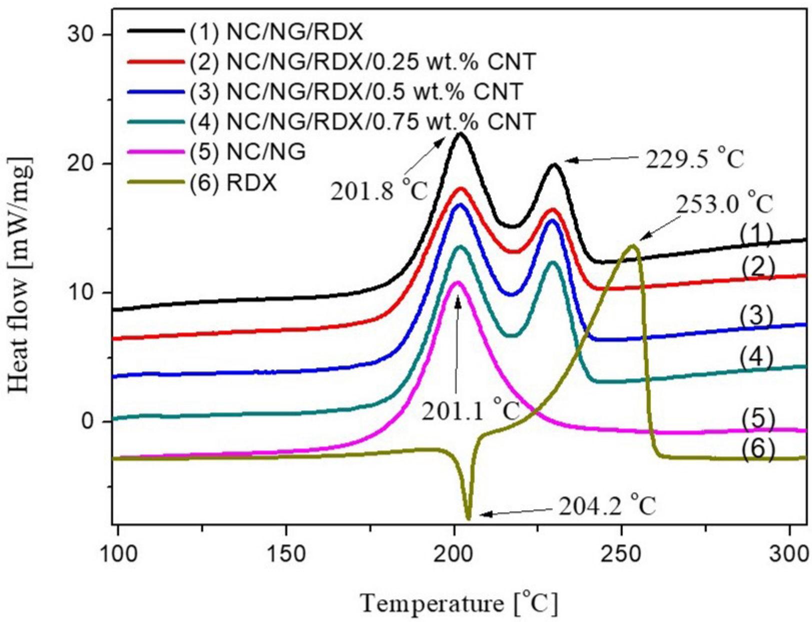

Figure 3. DSC curves of RDX, NC/NG and NC-NG-RDX propellants doped with and without CNTs

3.3 Near infrared light absorption

Figure 4 represents the near infrared light reflectivity property of NC-NG-RDX propellants with different contents of CNTs. Due to the similar processing used, the propellants obtained had similarly smooth surface structure which resulted in similar scattering and reflection of light [36]. Besides, the transmissivity of near infrared light in NC-NG-RDX propellants is very low. Therefore, near infrared light absorption for the propellants in this experiment can be revealed by the reflectivity spectra in Figure 4, which is determined by the incorporation of CNTs. As shown in Figure 4, with the increase of CNT content, the original reflectivity characteristics of the raw propellant gradually disappeared and the curves became smoother. At 800 nm, the light reflectivity for NC-NG-RDX propellant is 75.5%. However, the light reflectivity for NC-NG-RDX propellants containing CNTs clearly decreased with increasing CNT content, and the light reflectivities were 71.1%, 38.3% and 32.3% for the propellants containing 0.25, 0.5 and 0.75 wt.% of CNTs, respectively. Therefore, the near infrared light absorption performance of NC-NG-RDX propellants can be improved by a small amount of CNT, and is obviously enhanced by the incorporation of CNTs.

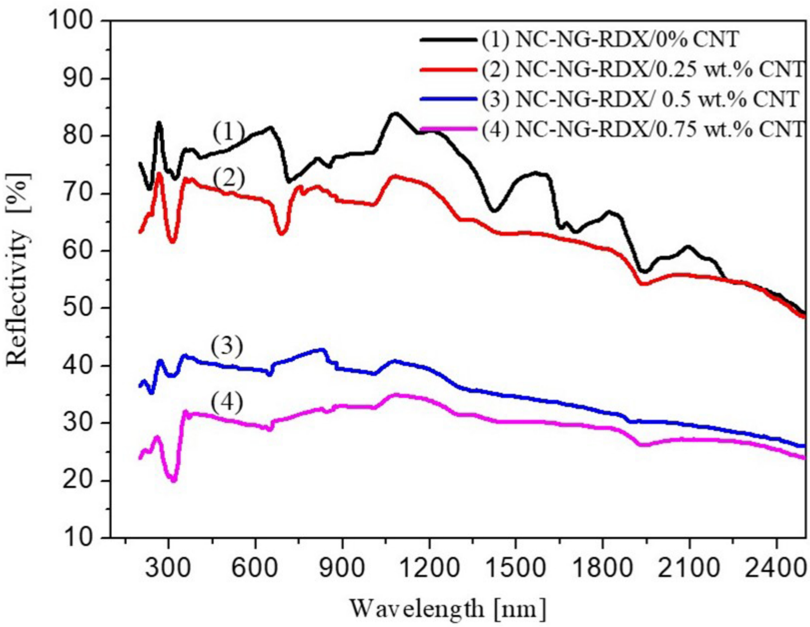

Figure 4. UV-visible-near infrared light reflectivity spectra of NC-NG-RDX propellants doped with and without CNTs

3.4 Thermal conductivity

Multi-walled CNTs with long aspect ratios have excellent thermal conductivity, and are often used as thermal conductive fillers to fabricate high thermal conductivity composite materials [37]. According to Figure 5, NC-NG-RDX propellants have a poor thermal conductivity of about 0.25 W/(m·K) at 25 °C. After addition of 0.25, 0.5 and 0.75 wt.% of CNTs, the thermal conductivity of NC-NG-RDX propellants increases by 3.6%, 13.6% and 16.8%, respectively. No substantial increase in thermal conductivity is attributed to a low content of CNTs [38]. In addition, when the test temperature increases from 25 to 100 °C, the thermal conductivity of NC-NG-RDX propellants increases by 12.2% on average. Therefore, the conductivities of the propellants with different CNT contents do not show much difference before and after a laser pulse is applied, and the variation of thermal conductivities may not be the major factor to tune the laser ignition performance of the propellants.

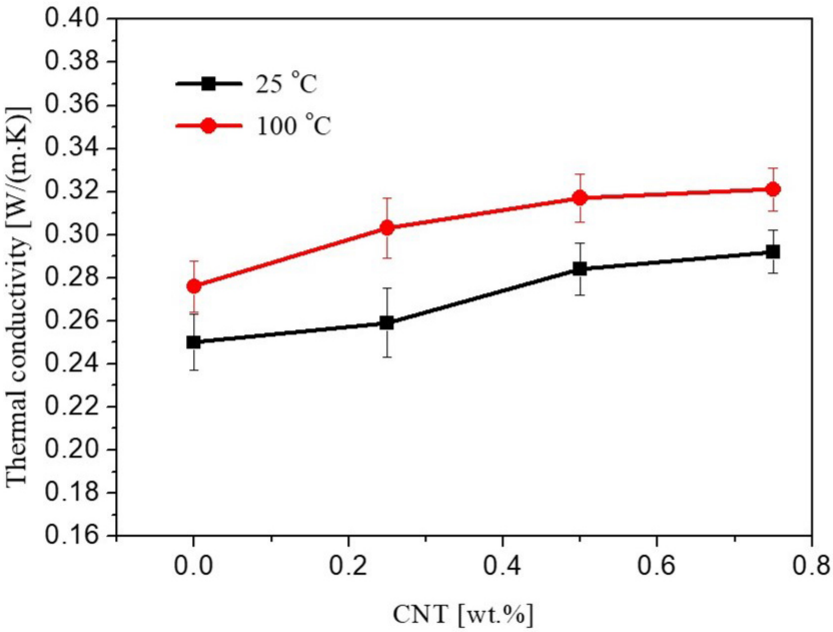

Figure 5. Thermal conductivity of NC-NG-RDX propellants with different content of CNTs at 25 and 100 °C

3.5 Laser ignition performance

The work of Courty *et al.* [22] shows that a coating of graphite considerably decreases the ignition energy values of NC-RDX propellants. However, the relationship between the ignition performance and the amount of optically sensitive additive was not indicated. Here, Figure 6 shows typical oscilloscope traces of the laser pulse and the ignited flame during the ignition and combustion of propellants doped with different CNT contents. 'First ignition' or ignition delay is the time when the first detected flame occurs. 'Successful ignition' is the time when an efficient deflagration appears before a self-sustained combustion. 'First ignition' and 'successful ignition' of the ignited propellants are marked by arrows in Figure 6. As shown in Figure 6(a), no obvious flame is detected even when the laser pulse time is more than 2 s, and a deflagration begins at about 2.1 s, which is followed by the successful ignition of NC-NG-RDX propellant. Propellants doped with 0.25 wt.% of CNTs show a different ignition performance compared with the raw propellant. According to Figure 6(b), the ignited flame first appears at 1.55 s, and then becomes weaker at 1.82 s. However, a strong flame suddenly appears at 2.02 s, and after that, stable combustion of the propellant is observed. As shown in Figure 6(c), the first ignition and successful ignition of propellant doped with 0.5 wt.% of CNTs are 0.02 and 0.45 s, respectively, and are much shorter than that of propellant doped with 0.25 wt.% of CNTs. In addition, a pulse time of 1 s is appropriate for laser ignition of this propellant. Therefore, the laser ignition performance of NC-NG-RDX propellants can be improved by incorporation of a small amount of CNT.

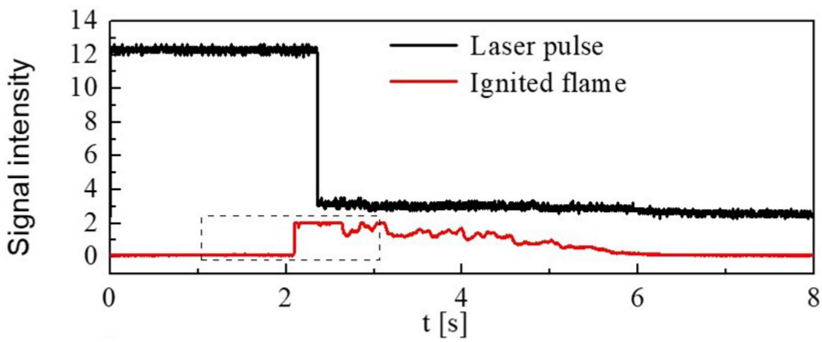

(a1)

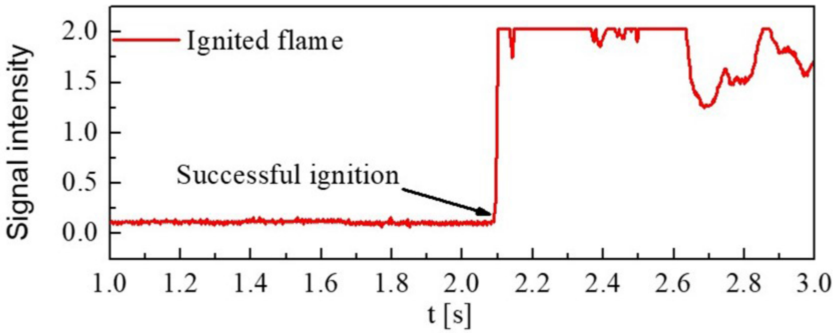

Ignited flame
Successful ignition
Signal intensity
t [s]

(a2)

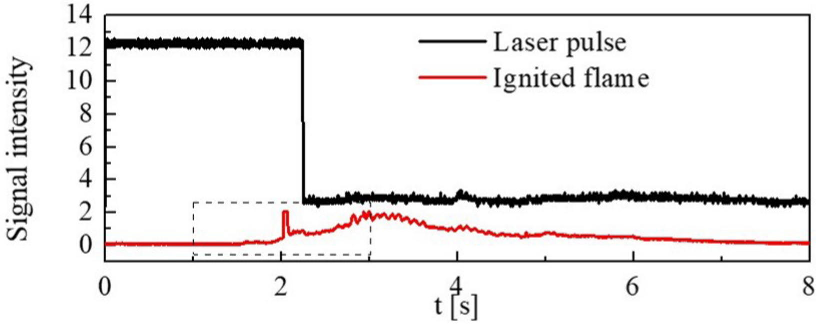

Laser pulse
Ignited flame
Signal intensity
t [s]

(b1)

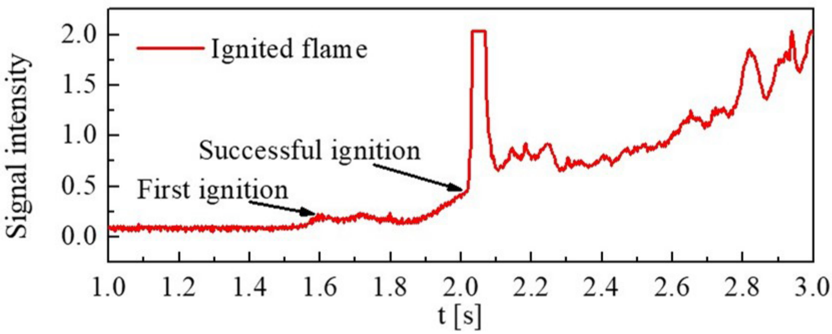

Ignited flame
Successful ignition
First ignition
Signal intensity
t [s]

(b2)

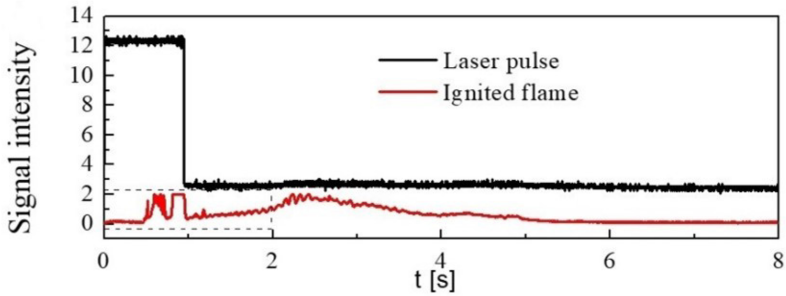
Signal intensity
Laser pulse
Ignited flame
t [s]

(c1)

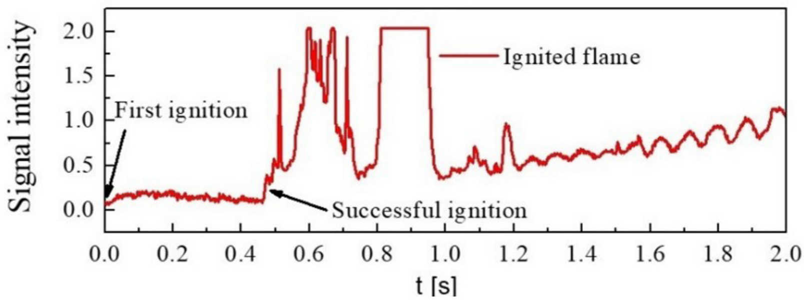
Signal intensity
Ignited flame
First ignition
Successful ignition
t [s]

(c2)

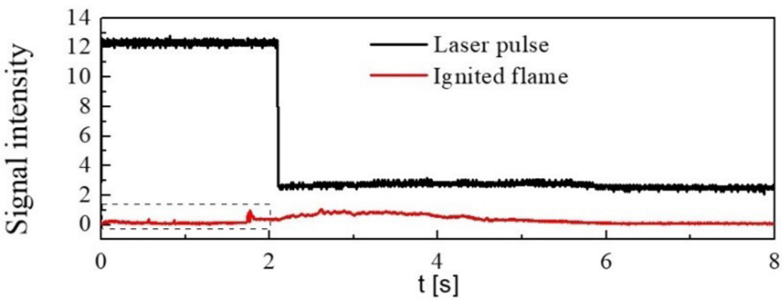
Signal intensity
Laser pulse
Ignited flame
t [s]

(d1)

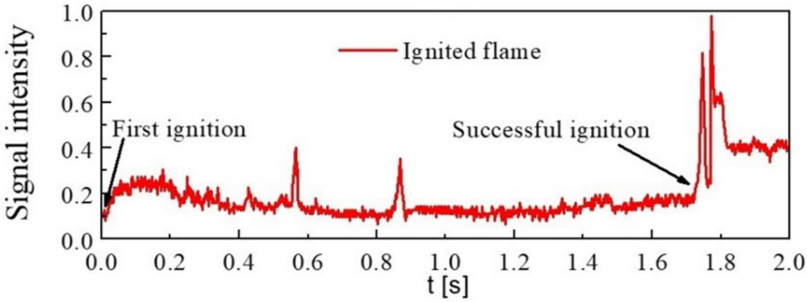

(d2)

Figure 6. Typical oscilloscope traces of laser pulse and the ignited flame during the ignition and combustion of NC-NG-RDX propellants: 0% CNTs (a), 0.25 wt.% (b), 0.5 wt.% (c), and 0.75 wt.% (d)

However, an interesting result of successful ignition is found for propellant doped with 0.75 wt.% CNTs. As shown in Figures 6(d1) and 6(d2), successful ignition of this sample increases by 1.26 s compared to propellant doped with 0.5 wt.% CNTs, even though its ignition time is only 0.01 s. As shown in Figure 6(d2), an ignited flame is detected immediately once the laser pulse works. However, the intensity of the ignited flame decreases slowly and no effective deflagration appears, even though the laser pulse was on continuously between 0 and 1.71 s. Eventually the propellants were penetrated by the laser beam, and ignited by the hot surroundings at 1.71 s. Due to the weak flame intensity during ignition, flameout, or unsuccessful ignition often occurs during several laser ignition tests of the propellant doped with 0.75 wt% CNTs. These results reveal that the laser ignition efficiency of the NC-NG-RDX propellant could be inhibited by an excess of photosensitive additive, such as 0.75 wt.% of CNTs or more.

Table 2. Ignition time and successful ignition time of NC-NG-RDX propellants doped with different CNT contents

Sample	1	2	3	4
CNT [wt.%]	0	0.25	0.50	0.75
First ignition time [s]	2.10	1.55	0.02	0.01
Successful ignition time [s]	2.10	2.02	0.45	1.71

3.6 Laser ignition mechanism

The laser power density used in this experiment was just about 700 W·cm^{-2} and the laser wavelength used was not the characteristic absorption wavelength of NC/NG/RDX propellant. Hence the effect of the laser beam on the NC-NG-RDX propellants is mainly due to heating [39]. During the laser beam heating process, there are several reactions in the irradiated propellant including decomposition of NC/NG, melting and volatilization of RDX, and decomposition of RDX. Inflammable gaseous products are generated by these reactions and accumulate on the surface of the irradiated propellant [1, 16, 17].

As shown in Figure 7, the gaseous products are ignited when the temperature (T) reaches the critical ignition temperature (T_c) according to the thermal mechanism of laser ignition. In Figure 7, W, α, t and ΔH_p, are the laser power, laser absorption efficiency, irradiation time and heat released by decomposition of the irradiated propellant, respectively. However, only if the heat released by the combustion of the gaseous products (ΔH_c) reaches the ignition energy threshold of the propellant samples (Q_i), can a successful laser ignition be realized. In addition, due to the similar morphology and components, T_c and Q_i of the propellant samples can be considered consistent. Consequently, laser ignition of NC-NG-RDX propellants is determined by both the temperature of the irradiated region and the heat released by the deflagration of the decomposition products produced by the irradiated propellants.

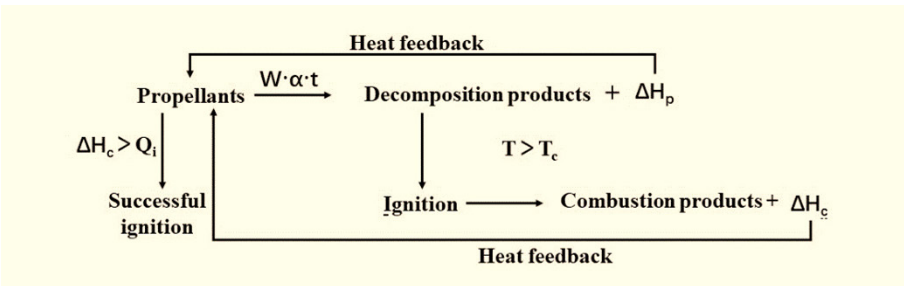

Figure 7. Schematic diagram of the laser ignition of NC-NG-RDX propellants

Figure 8 represents the hypothetical laser ignition mechanism of both NC-NG-RDX propellants and NC-NG-RDX propellants doped with 0.75 wt.% CNTs. Figures 8(a) to 8(g) are the description of the figures in Figure 8(1) and Figure 8(2), and the deeper red of liquid reaction regions represents a higher temperature. As shown in Figure 8(1), there is a liquid reaction region (Figure 8(b)) in the irradiated region of the propellants at the beginning of the laser pulse (Figure 8(a)). The liquid reaction region is generated by the decomposition of NC-NG and the melting of RDX particles. The infrared light reflectivity of NC-NG-RDX propellants (Figure 8(d)) is 75.5%. Therefore the absorption of laser energy in the irradiated region is inefficient. At the same time, melting of high content RDX particles in the propellant further consumes the absorbed laser energy. So, the temperature of the liquid reaction rises slowly together with extension of the liquid reaction region and the accumulation of inflammable gas (Figure 8(c)). Once the temperature reaches the ignition point, large quantities of the gaseous products are first ignited. The energy released by the chemical reaction should be greater than the ignition threshold of the propellants, and the ignition is successful.

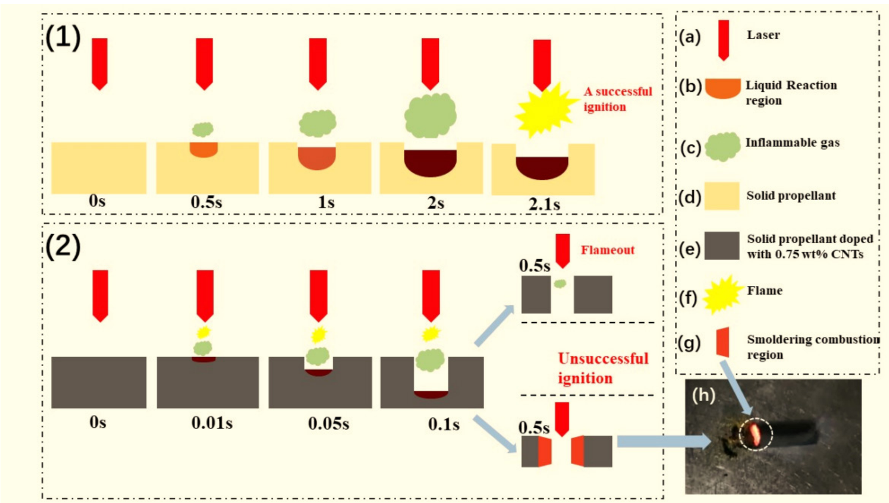

Figure 8. Schematic illustration of laser ignition mechanism of NC-NG-RDX propellants (1) and NC-NG-RDX propellant with 0.75 wt.% CNTs (2)

The most significant effect of the incorporation of CNTs into NC-NG-RDX propellants is the decrease of the laser reflectivity due to the excellent laser absorption of CNTs [27]. As shown in Figure 4, the laser reflectivity decreased by 5.8%, 49.3% and 57.2% as compared to the value for 0% CNT as the CNT content was increased from 0.25 to 0.75 wt.%. The improvement of laser absorption obviously enhances the heating rate of the liquid region of the propellants. As shown in Table 2, first ignition time or ignition delay time decreased from 2.1 to 0.01 s. However, excessive laser absorption or heating rate is not conducive to a successful ignition, as shown in Figures 6(d1) and 6(d2), and the mechanism is explained in Figure 8(2). According to previous studies, the interaction region between the laser and the propellants is quite thin due to the low penetrability of infrared laser [40]. Due to the high heating rate and thin size, the interaction region decomposed and gaseous products were ignited quickly. However, the energy released by the chemical reaction cannot reach the Q_i of the propellants. Therefore, liquid reaction region in Figure 8(2) is quite thin or almost non-existent, and the interaction region rapidly extended in the direction of the laser beam. The propellants can be penetrated quickly by the laser and flame out or smoldering combustion (Figures 8(g) and 8(h)) followed. As a result, there is only an appropriate laser absorption efficiency to ignite the propellants, and 0.5 wt.% is the optimum content for CNTs to tune the direct laser ignition performance of NC-NG-RDX propellants.

4 Conclusions

- In this study, the effect of the presence of CNTs on the infrared laser ignition characteristics of NC-NG-RDX propellants with 40 wt.% of RDX has been investigated in an atmospheric environment. NC-NG-RDX propellants with 0 to 0.75 wt.% of CNTs were prepared using an ultrasonic and kneading method, and CNTs and RDX particles were dispersed uniformly.
- NC-NG-RDX propellants show a two-step decomposition including the decomposition of NC-NG, and melting and decomposition of RDX particles. The decomposition property of the propellant is not changed by the presence of a low content of CNTs. Meanwhile, the thermal conductivity increased slightly with increase of CNT content. The laser reflectivity of the propellant decreased by 5.8%, 49.3% and 57.2% as the CNT content was increased from 0.25 to 0.75 wt.% due to the excellent laser absorption of CNTs.
- The propellants became more sensitive to laser and the first ignition time decreased from 2.1 to 0.01 s. However, the addition of excessive CNTs (0.75 wt.%) suppressed successful ignition of the propellants by high laser absorption, sharp heating rate and rapid decomposition of the irradiated region and lack of effective deflagration.
- These results suggest that an appropriate proportion of CNTs could potentially be used as a laser sensitizer for realizing an effective infrared laser ignition of NC-NG-RDX propellants. Incorporation of a small amount of carbon nanomaterial is a convenient and promising method to improve the laser ignition property of RDX based propellants at infrared wavelength, or even at other wavelengths.

Conflict of interest

The authors declare no conflict of interest, financial or otherwise.

Acknowledgements

This work was supported by the Project of State Key Laboratory of Environment-friendly Energy Materials of Southwest University of Science and Technology (No. 20fksy18).

References

[1] Liau, Y.C.; Kim, E.S.; Yang, V.A Comprehensive Analysis of Laser-induced Ignition of RDX Monopropellant. *Combust. Flame* **2001**, *126*(3):1680-1698.
[2] Saito, T.; Shimoda, M.; Yamaya, T.; Iwama, A. Ignition of AP-based Composite Solid Propellants Containing Nitramines Exposed to CO_2 Laser Radiation at sub Atmospheric Pressures. *Combust. Flame* **1991**, *85*(1-2): 68-76.
[3] Ilyushin, M.A.; Tselinskii, I.V. The Influence of the Structure of the Salts of Azoles upon the Processes of Their Thermal and Laser Initiation. *Cent. Eur. J. Energ. Mater.* **2006**, *3*(1-2): 39-50.
[4] Nakayama, H.; Miyashita, T.; Hashino, S.; Yoshitake, N.; Orita, R. An Approximate Theory of Laser-induced Ignition of Boron/Potassium Nitrate Pyrotechnic. *Sci. Technol. Energ. Mater.* **2010**, *71*(1): 31-38.
[5] Sumpter, D.R. Laser-Initiated Ordnance for Air-to-Air Missiles. *Proc. 29th* Joint Propulsion Conference and Exhibit, Monterey, US, **1993**, AIAA-93-2360, 137-147.
[6] Barrows, A.W.; Forch, B.E.; Chang, L.M.; Howard, S.L.; Beyer, R.A. Laser Ignition Testing of Two-Piece Tank Ammunition for Advanced Tank Cannon System (ATACS). *AD-A283628, ARL-TR-474*, **1994**.
[7] Khaneft, A.V.; Duginov, E.V. Effect of Melting on the Critical Ignition Energy of Condensed Explosives by a Short Laser Pulse. *Combust., Explos. Shock Waves* **2012**, *48*(6): 699-704.
[8] Lavid, M.; Gulati, S.K.; Lempert, W.R. Laser Ignition of Ball Powder (Nitrocellulose base). *Proc. SPIE* **1994**, *2122*: 129-143.
[9] O'Briant, S.A.; Gupta, S.B.; Vasu, S.S. Review: Laser Ignition for Aerospace Propulsion. *Propuls. Power Res.* **2016**: 1-21.
[10] Carleton, F.B.; Klein, N.; Krallis, K.; Weinberg, F.J. Laser Ignition of Liquid Propellants. *Proc. Symp. (Int.) Combustion* **1991**, *23*(1): 1323-1329.
[11] Wu, X.J.; Rao, G.N.; Chen, L.P.; Chen, W.H.; Wang, J.N.; Zhang, C.N. Analysis for Decomposition Characteristics and Piecewise Thermokinetics of Nitramine Modified Double-base Propellant with High Solid Content. *Propellants Explos. Pyrotech.* **2017**, *42*: 1-7.
[12] Mcdonald, B.A. Study of the Effects of Aging under Humidity Control on the Thermal Decomposition of NC/NG/BTTN/RDX Propellants. *Propellants Explos.*

Pyrotech. **2011**, *36*(6): 576-583.
[13] Liu, R.; Zhang, T.L.; Yang, L.; Zhou, Z.N. Dynamic Pressure Thermal Analysis of Double-base Propellants Containing RDX. *Centr. Eur. J. Chem.* **2014**, *12*(6): 672-677.
[14] Isbell, R.A.; Brewster, M.Q. Optical Properties of Energetic Materials: RDX, HMX, AP, NC/NG, and HTPB. *Propellants Explos. Pyrotech.* **1998**, *23*(4): 218-224.
[15] Zhang, X.; Hikal, W.; Zhang, Y.; Bhattcacharia, S.; Li, L.; Wang, S.R.; Weeks, B.L. Direct Laser Initiation and Improved Thermal Stability of Nitrocellulose/Graphene Oxide Nanocomposites. *Appl. Phys. Lett.* **2013**, *102*(14): 5428.
[16] Ulas, A.; Kuo, K.K. Laser-induced Ignition of Solid Propellants for Gas Generators. *Fuel* **2008**, *87*(6): 639-646.
[17] Li, L.B.; Chen, X.; Zhou, C.H.; Zhu, M.; Musa, O. Experimental Investigation on Laser Ignition and Combustion Characteristics of NEPE Propellant. *Propellants Explos. Pyrotech.* **2017**, *42*(9): 1-10.
[18] Ahmad, S.R.; Russell, D.A.; Leach, C.J. Studies into Laser Ignition of Unconfined Propellants. *Propellants Explos. Pyrotech.* **2001**, *26*(5): 235-245.
[19] Ahmad, S.R.; Russell, D.A. Laser Ignition of Pyrotechnics-Effects of Wavelength, Composition and Confinement. *Propellants Explos. Pyrotech.* **2005**, *30*(2): 131-139.
[20] Liu, C.J.; Li, X.D.; Li, R.; Yang, Q.; Zhang, H.P.; Yang, B.; Yang, G.C. Laser Ignited Combustion of Graphene Oxide/Nitrocellulose Membrane for Solid Propellant micro Thruster and Solar Water Distillation. *Carbon* **2020**, *166*: 138-147.
[21] Li, X.D.; Huang, B.; Li, R.; Zhang, H.P.; Qin, W.Z.; Qiao, Z.Q.; Liu, Y.S.; Yang, G.C. Laser-Ignited Relay-Domino-Like Reactions in Graphene Oxide/CL-20 Films for High-Temperature Pulse Preparation of Bi- Layered Photothermal Membranes. *Small* **2019**, 1900338.
[22] Courty, L.; Gillard, P.; Ehrhardt, J.; Baschung, B. Experimental Determination of Ignition and Combustion Characteristics of Insensitive Gun Propellants based on RDX and Nitrocellulose. *Combust. Flame* **2021**, *229*: 111402.
[23] Fang, X.; Sharma, M.; Stennett, C.; Gill, P.P. Optical Sensitisation of Energetic Crystals with Gold Nanoparticles for Laser Ignition. *Combust. Flame* **2017**, *183*: 15-21.
[24] Bayat, Y.; Malmir, S.; Hajighasemali, F.; Dehghani, H. Reductive Debenzylation of Hexabenzylhexaazaisowurtzitane Using Multi-walled Carbon Nanotube-supported Palladium Catalysts: An Optimization Approach. *Cent. Eur. J. Energ. Mater.* **2015**, *12*(3): 439-458.
[25] Denisyuk, A.P.; Milekhin, Y. M.; Demidova, L.A.; Sizov, V.A. Effect of Carbon Nanotubes on the Catalysis of Propellant Combustion. *Dokl. Chem.* **2018**, *483*(2): 301-303.
[26] Ajayan, P.M.; Terrones, M.; De la Guardia, A.; Huc, V.; Grobert, N.; Wei, B.Q.; Lezec, H.; Ramanath, G.; Ebbesen, T.W. Nanotubes in a Flash Ignition and Reconstruction. *Science* **2002**, *296*(5568): 705.
[27] Kim, J.H.; Ahn, J.Y.; Park, H.S.; Kim, S.H. Optical Ignition of Nanoenergetic Materials: The Role of Single-walled Carbon Nanotubes as Potential Optical

Igniters. *Combust. Flame* **2013**, *160*(4): 830-834.
[28] Tseng, S.H.; Tai, N.H.; Hsu, W.K.; Chen, L.J.; Wang, J.H.; Chiu, C.C.; Chi, Y.L.; Chou, L.J.; Leou, K.C. Ignition of Carbon Nanotubes Using a Photoflash. *Carbon* **2007**, *45*(5): 958-964.
[29] Kim, J.H.; Cho, M.H.; Kim, K.J.; Kim, S.H. Laser Ignition and Controlled Explosion of Nanoenergetic Materials: The Role of Multi-walled Carbon Nanotubes. *Carbon* **2017**, *118*: 268-277.
[30] Kim, J.H.; Kim, S.B.; Choi, M.G.; Kim, D.H.; Kim, K.T.; Lee, H.M.; Lee, H.W.; Kim, J.M.; Kim, S.H. Flash-ignitable Nanoenergetic Materials with Tunable Underwater Explosion Reactivity: The Role of Sea Urchin-like Carbon Nanotubes. *Combust. Flame* **2015**, *162*(4): 1448-1454.
[31] Manaa, M.R.; Mitchell, A.R.; Garza, R.G.; Pagoria, P.F.; Watkins, B.E. Flash Ignition and Initiation of Explosives-Nanotubes Mixture. *J. Am. Chem. Soc.* **2005**, *127*(40):13786.
[32] Shen, J.P.; Liu, Z.T.; Xu, B.; Liang, H.; Zhu, Y.; Liao, X.; Wang, Z.S. Influence of Carbon Nanofibers on Thermal and Mechanical Properties of NC-TEGDN-RDX Triple-base Gun Propellants. *Propellants Explos. Pyrotech.* **2019**, *44*: 355-361.
[33] Shen, J.P.; Liu, Z.T.; Xu, B.; Chen, F.Y.; Zhu, Y.; Fu, Y.; Kline, D.J.; Liao, X.; Wang, Z.S. Tuning the Thermal, Mechanical, and Combustion Properties of NC-TEGDN-RDX Propellants via Incorporation of Graphene Nanoplates. *J. Energ. Mater.* **2020**, *38*(3): 326-335.
[34] Herreros, D.N.; Fang, X. Laser Ignition of Elastomer-modified Cast Double-base (EMCDB) Propellant Using a Diode Laser. *Opt. Laser Technol.* **2017**, *89*: 21-26.
[35] Jing, W.W.; Dang, Z.M.; Yang, G.P. The Thermal Decomposition Behavior of RDX-base Propellants. *J. Therm. Anal. Calorim.* **2005**, *79*(1): 107-113.
[36] Wang, X.; Liu, Q.C.; Wu, S.Y.; Xu, B.X.; Xu, H.X. Multilayer Polypyrrole Nanosheets with Self-organized Surface Structures for Flexible and Efficient Solar-Thermal Energy Conversion. *Adv. Mater*. **2019**, *31*(19) paper 1807716: 1-9.
[37] Kumanek, B.; Janas, D. Thermal Conductivity of Carbon Nanotube Networks: A Review. *J. Mater. Sci.* **2019**, *54*: 7397-7429.
[38] Han, Z.D.; Fina, A. Thermal Conductivity of Carbon Nanotubes and Their Polymer Nanocomposites: A Review. *Prog. Polym. Sci.* **2011**, *36*(7): 914-944.
[39] Ritchie, S.J.; Thynell, S.T.; Kuo, K.K. Modeling and Experiments of Laser-induced Ignition of Nitramine Propellants. *J. Propul. Power* **1997**, *13*(3): 367-374.
[40] Damm, D.; Maiorov, M. Thermal and Radiative Transport Analysis of Laser Ignition of Energetic Materials. *Proc. SPIE* **2010,** 7795: 779502.

Received: April 19, 2021
Revised: September 27, 2021
First published online: September 30, 2021